

Oumeng Zhang, Jin Lu, Tianben Ding, and Matthew D. Lew

Electrical and Systems Engineering, Washington University in St. Louis, St. Louis, Missouri 63130, USA

In the original paper,¹ a calibration error exists in the image-formation model used to analyze experimental images taken by our microscope, causing a bias in the orientation measurements in Figs. 2 and 3. The updated measurements are shown in Fig. E1; Figs. E1(a) and E1(b) correspond to the original Figs. 2(c) and 2(d); Figs. E1[c(i)] and E1[d(i)] correspond to the γ estimates in the original Figs. 3[a(iii)] and 3[b(iii)]; Figs. E1[c(ii)] and E1[d(ii)] correspond to the original Figs. 3[a(iv)] and 3[b(iv)]. We have also updated the supplementary material to discuss the revised PSF model and estimation algorithms (supplementary material 2) and show the revised model and measurements (Figs. S1, S3, S7, S8, and S10–S13).

The precise error is a flipped coordinate system in the back focal plane of the y -polarized imaging channel [Figs. S1 and S3(i)], resulting in changes to the XY and XZ basis images [Figs. S3(v) and S3(vi)]; no other basis images are affected. This correction has a negligible effect on the orientation measurements of Atto 647N embedded in polymethyl methacrylate; Fig. 1 of the original paper is unchanged.

For fluorescent beads embedded in polyvinyl alcohol, we measure a smaller effective rotational constraint [Fig. E1(a)] for both 20-nm (mean $\gamma = 0.37$) and 100-nm (mean $\gamma = 0.30$) beads than originally reported. This correction does not change any of the conclusions of the original paper, e.g., 20-nm beads exhibit a larger rotation in their second-moment vectors M (mean $\hat{\delta} = 0.32$) than 100-nm beads (mean $\hat{\delta} = 0.06$) after a 90° rotation in pumping polarization.

For Atto 647N molecules embedded in polyvinylpyrrolidone exposed to humid air, our measurements of rotational constraint over 50 min are modestly affected {Figs. E1[c(i)] and E1[d(i)]}. Despite a significant correction to the orientation trajectories of molecules 1 {Fig. E1[c(ii)]} and 2 {Fig. E1[d(ii)]}, we still find that molecules with smaller effective rotational constraints [$\gamma = 0.98 \pm 0.05$ (mean \pm std.) and equivalent cone half angle of $\alpha = 9^\circ$ for molecule 1 within a single frame] may exhibit smaller slow-scale rotations over long timescales (28° for molecule 1 over 50 min) than those with larger constraints [mean $\gamma = 0.99 \pm 0.02$ ($\alpha = 5^\circ$) within a frame and a rotation of 37° over 50 min for molecule 2].

REFERENCES

¹O. Zhang, J. Lu, T. Ding, and M.D. Lew, Appl. Phys. Lett. **113**, 031103 (2018).

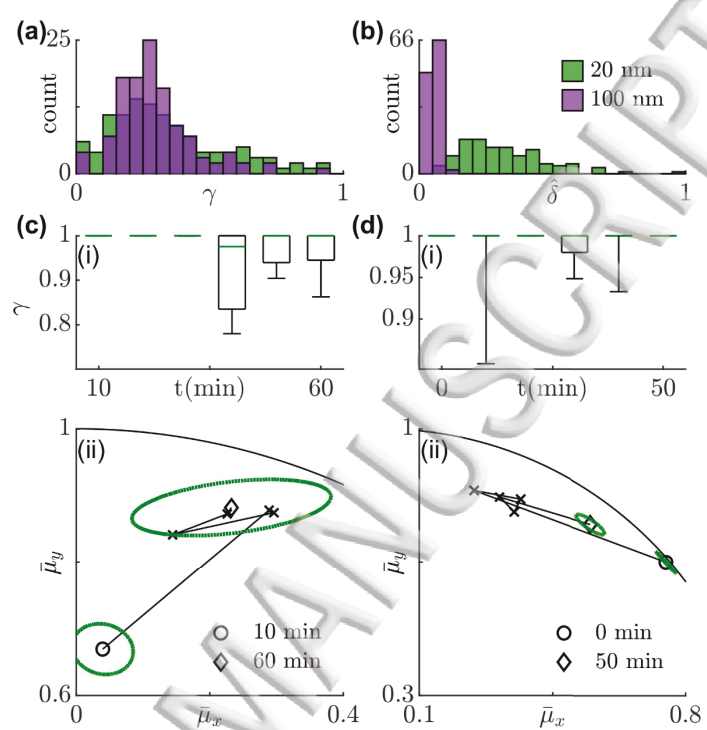


Fig. E1. (a) Rotational constraint γ and (b) normalized rotation $\hat{\delta}$ in response to x - and y -polarized excitation of 118 fluorescent beads. Green, 20-nm beads; purple, 100-nm beads. For (c) molecule 1 and (d) molecule 2, measurements of (i) effective rotational constraint γ and (ii) their orientation trajectories over 50 min. Circle and diamond represent the beginning and end of the time-lapse measurement. Dashed green ellipse represents the covariance matrix in the estimated orientation $(\bar{\mu}_x, \bar{\mu}_y)$ measured at the beginning and end points. Solid curve marks the orientation domain $\bar{\mu}_x^2 + \bar{\mu}_y^2 \leq 1$.

